SAND2000-0577C

Two Target Height Effects on Interferometric Synthetic Aperture Radar Coherence

David A. Yocky* and Charles V. Jakowatz, Jr.

Sandia National Laboratories, P.O. Box 5800, MS1207, Albuquerque, NM 87185-1207

ABSTRACT

Useful products generated from interferometric synthetic aperture radar (IFSAR) complex data include height measurement, coherent change detection, and classification. The IFSAR coherence is a spatial measure of complex correlation between two collects, a product of IFSAR signal processing. A tacit assumption in such IFSAR signal processing is that one height target exists in each range-Doppler cell. This paper presents simulations of IFSAR coherence if two targets with different heights exist in a given range-Doppler cell, a condition in IFSAR collections produced by layover. It also includes airborne IFSAR data confirming the simulation results. The paper concludes by exploring the implications of the results on IFSAR classification and height measurements.

Keywords: Interferometric SAR, coherence, layover

1. INTRODUCTION

Conventional synthetic aperture radars (SAR) are active microwave systems usually operating in the 250-MHz to 50-GHz range. The return radiation is captured as complex wavefront data containing both amplitude and phase information. Dual-pass collections or dual-antenna systems allow the comparison or interference of the two or more complex data sets. This interferometric SAR exploitation generates products like topographic measurements,[1-6] coherent change detection,[6,7] and land-cover classification.[8-11]

The fundamental measure of the ability to interfere two SAR collects is the coherence expressed as

$$\gamma = \frac{\left| \sum_i \sum_j g_{ij}^* \cdot h_{ij} \right|}{\sqrt{\sum_i \sum_j |g_{ij}|^2 \cdot \sum_i \sum_j |h_{ij}|^2}} \tag{1}$$

where g_{ij}^* is the complex conjugate of the first image, h_{ij} is the second complex image, both for the ith range index and the jth azimuth index, and the summation is over the number of complex looks. The coherence is a correlation estimate and is analogous to the optical complex coherence factor.[12] A totally coherent pair of images would be a matrix of ones while any drop in coherence would be values less than unity.

Interferometric SAR (IFSAR) processed products are intimately linked to the coherence of two or more images on a pixel by pixel basis. For instance, the phase difference measurements for IFSAR topography is sensitive to the coherence of each pixel. Low coherence values suggest the targets have changed between collects (dual-pass), or the antennas received different signals from the same target due to quickly changing targets or geometry-dependent scattering (dual-antenna). IFSAR topography generation assumes the SAR complex reflectance will be similar between collects or between antennas to extract the height information. Slightly dissimilar complex reflectance causes a decrease in coherence and injects noise errors into the final height calculations.

* Correspondence: Email: dayocky@sandia.gov; Telephone: 505 844 5188; FAX: 505 844 8648

DISCLAIMER

While height measurements are of interest in IFSAR exploitation, targets with height relief have other properties. Fundamental SAR imaging characteristics cause targets with height relief to appear at a closer range than they actually occur in the ground plane. Thus, this relief may lay over onto other targets with different heights and reflection characteristics. This paper examines how lay over of two targets affects the coherence by modeling such targets with a SAR synthetic target generator. These simulated results are compared to airborne IFSAR complex imagery capturing the two-target height coherence effect. We also examine the implications on IFSAR topography and classification products.

2. TWO-HEIGHT COHERENCE: TARGET SIMULATION

Due to lay over, more than one target can occupy a given SAR range resolution cell at a given azimuth (Doppler) sample. The range cell will then contain a complex reflectance that is a mixture of the targets present. While a distribution of targets could fit into this scenario, we simplify by examining only two targets in a single range cell. We also present this scenario as a dual-antenna collection, although it can be a dual pass collection. The baseline, B, is the separation between antenna. We assume good system signal-to-noise ratio, no registration errors, no squint, and no surface tilts. Figure 1 shows typical collection geometry with a dual-antenna SAR and two point targets having different heights, 0 and z, occurring in a single range resolution cell, ρ. Δy is the layover in range, r_1 and r_2 are the ranges to the antennas, and the θs are the instantaneous depression angles.

The study of coherence characteristics as a function of baseline makes use of a synthetic target generator simulating a spotlight mode SAR collection. Table 1 contains the modeled parameters. Each image consists of 1828 point targets. There are four target groups as shown in Figure 2. 1) A background group representing flat ground with no height. This group is circular and the largest in number. 2) A single, point-target group with 5-m height simulating single, isolated trees. These single point targets lie on the cardinal (azimuth, range) axes and at 45-degree increments. 3) A 5-m height, sparsely populated square of targets to the left of scene center. This group models a sparse tree canopy. 4) A dense, 10-m height circular group at scene center intended to model tall, dense tree canopies. Thus, the simulation models single, sparse, and dense tree canopies each with single values of height. There is no attempt to model volume scattering or height variance. Each point target has a unique random phase. All targets have the same amplitude. There is no occlusion checking for shadow creation.

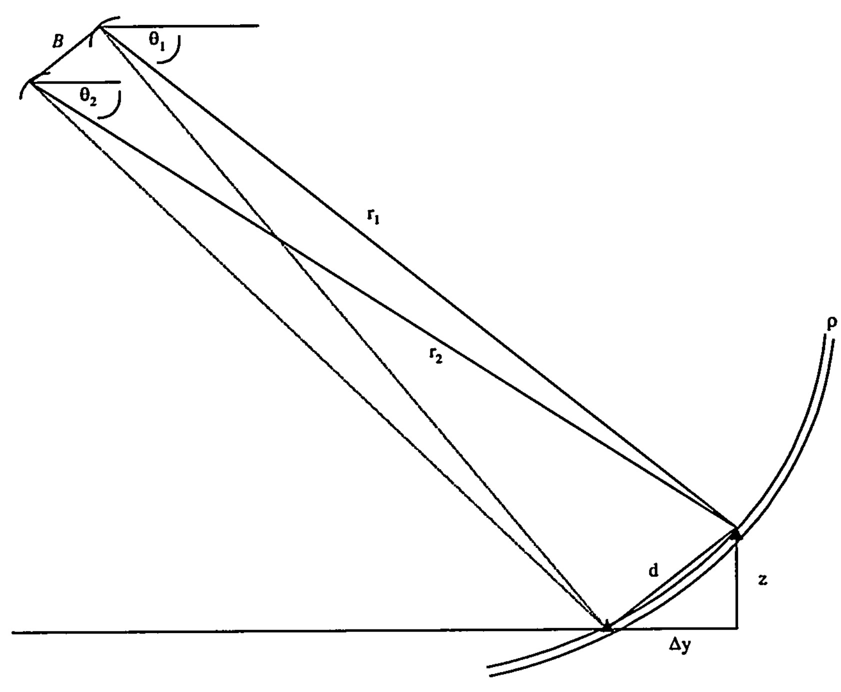

Figure 1. A dual antenna SAR collection geometry with targets of heights zero and z.

The complex imagery is formed in the ground plane using polar formatting after the addition of Gaussian noise to the complex data simulating a 20 dB signal-to-noise ratio. Figure 3a shows a synthetic image. In the middle of the image, the 10-m targets lay over on the ground targets. There exists a void, resembling a shadow, where no target returns exist. The rectangular-shaped 5-m targets are not distinguishable from the ground targets since there are no simulated shadows to distinguish the targets with height.

For the coherence modeling, each imaging step increments the vertical baseline by one meter and changes the depression angle such that the radar is always pointing at scene center. The imagery is formed using polar formatting and interfered with the first complex image. Calculation of the coherence uses a 3x3 box. Figures 3b-d show coherence results for various baselines.

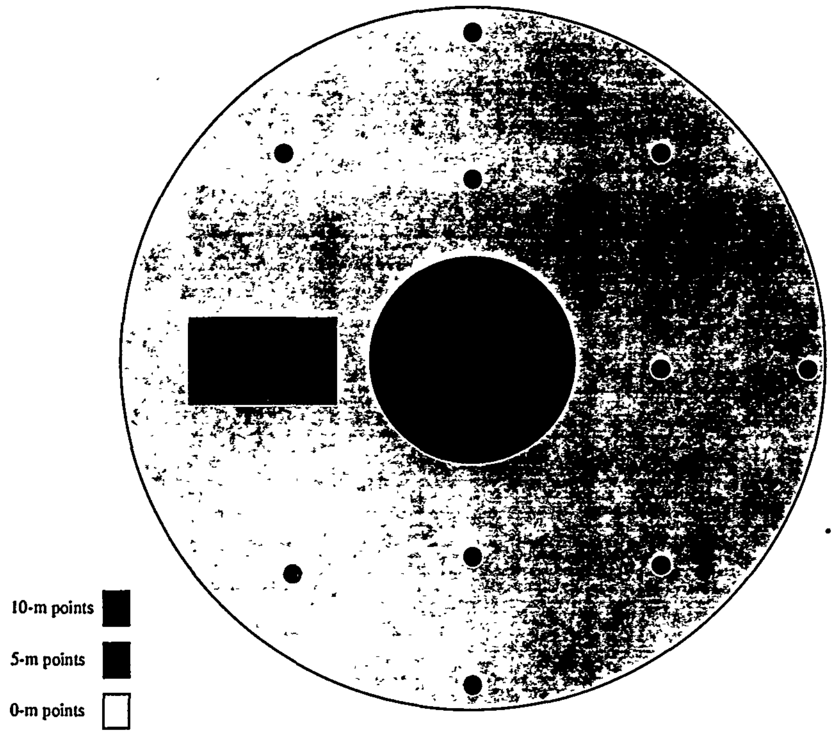

Figure 2. Simulation area setup.

Radar center frequency	1.0×10^{10} Hz
Transmitted bandwidth	3.8×10^{8} Hz
Chirp rate	1.0×10^{12} Hz/sec
Pulse repetition frequency	210.25 Hz
A-to-D sampling rate	1.81×10^{6} Hz
Radar platform velocity	100.0 m/s
Radar range to scene center	10.0 km
Radar depression angle	30.0 deg.
Collection angular subtense	1.96 deg.
Resolution (az, r)	0.45, 0.40 m
Ground plane pixel size (az, r)	0.31, 0.30 m
Slant plane patch diameter	200.0 m

Table 1 SAR Simulation Parameters.

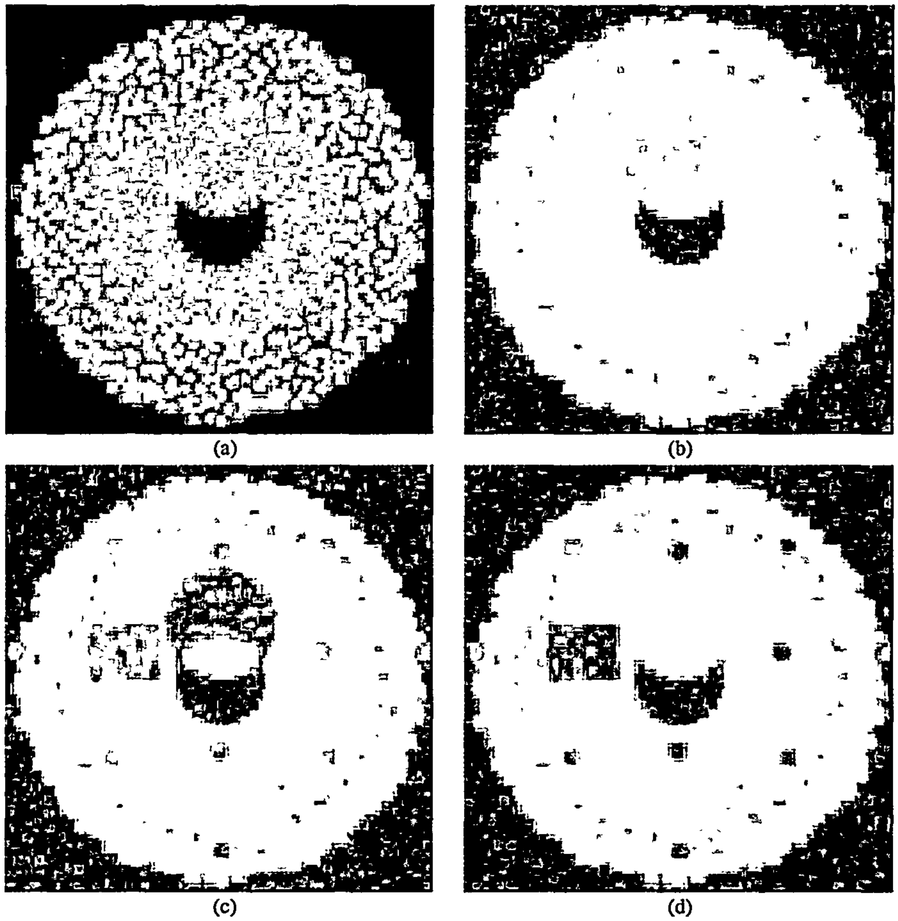

Figure 3-a) Log-enhanced SAR simulation magnitude image, b) Coherence map for 1-m vertical baseline. c) Coherence map for 5-m vertical baseline, and d) Coherence map for 11-m vertical baseline. Azimuth is the horizontal and range is the vertical direction. Near range is the top of each figure.

3. RESULTS

The simulation results suggest that a dense canopy, where SAR radiation does not reach the ground and volume scattering is negligible, will not have high coherence across the entire canopy. The simulation shows a portion of the dense canopy near the target shadow is most likely to have a single height target per range resolution cell, producing an area of high coherence. This is evident by the elliptical portion of the 10-m height group in the middle of Figures 3b,c, and d. These 10-m targets do not lay over on ground pixels, making them lone targets in their respective range resolution cells and highly correlated between antenna collections independent of height. However, the majority of the canopy coherence depends on target returns in the near-range because of the layover of the canopy onto these targets, a two-target-height coherence effect. This layover-dependent coherence is a function of height phase differences as well as the relative target strengths.

The simulated 10-m targets lose coherence, as a function of baseline, faster than the 5-m targets when both lay over onto ground targets as seen in Figures 3c and d. Other researchers have seen tall trees with low coherence while meadows have high coherence.[8-11] The fact that some larger baseline will cause the 10-m targets to become coherent again with the ground targets is significant. Figure 3d shows this. The results suggest if layover effects dominate, the choice of baseline will influence the coherence of the two-target case. Bickel *et al.*[13] predicted this two-target coherence effect.

Actual dual-antenna SAR data verify the simulation results. Figure 4a is the detected image of a storage tank collected by a 9.7 GHz airborne IFSAR with 0.3048-m resolution in range and azimuth. Figure 4b is the coherence map of the same storage tank from antennas on the airplane belly and wing. Note the layover portion of the storage tank has a distinct drop in coherence compared to the top of the storage tank, consistent with the simulated results in Figure 3c.

Figure 5a is the detect image of a dense tree canopy and single trees. Figure 5b shows the coherence map of the trees using belly and wing antenna. What is significant is the amount of high coherence in the dense canopy suggesting similar heights. Note also the drop in coherence on the near range (top of figure) edges of the canopy where the trees layover onto the ground.

The dual-antenna SAR data also verify the change in layover coherence as a function of baseline. Figure 6a is the detected image of the storage tank, a different collection than Figure 4a. Figure 6b is the coherence map of the storage tank. For this collection, the images are acquired from antenna on opposite wings, thus a larger baseline. Note the storage tank coherence in the layover portion is comparable to the coherence for the storage tank top. This coherence result is distinctly different from Figure 4b where the storage tank layover had lower coherence than the storage tank top. Figure 6b coherence result is similar to the simulated result in Figure 3d.

4. CONCLUSIONS

The two-height coherence phenomenon impacts the use of IFSAR coherence for classification. If the height-dependent coherence dominates volume or temporal coherence contributions, and the baseline values are much less than the critical baseline,[14] the coherence value will change as a function of baseline and/or target height. Picking the appropriate baseline value, trees could show higher or similar coherence compared to bushes or grass, which is contrary to coherence classification schemes that assume a drop in coherence as a function of class height. On the other hand, if object heights are a known constant, like standard telephone poles, the two-height coherence effect may assist classification.

The coherence characteristic discussed in this paper is useful in creating accurate IFSAR terrain maps. The characteristic shows areas where the SAR is receiving information from more than one target within the same range resolution cell. A measure of when more than one target per range resolution cell occurs is beneficial and has been used in height mapping urban areas and combining height data from multiple-pass and opposite-look IFSAR collections.[13] Using coherence, layover affected terms were dismissed and other heights selected resulting in a more accurate height maps.

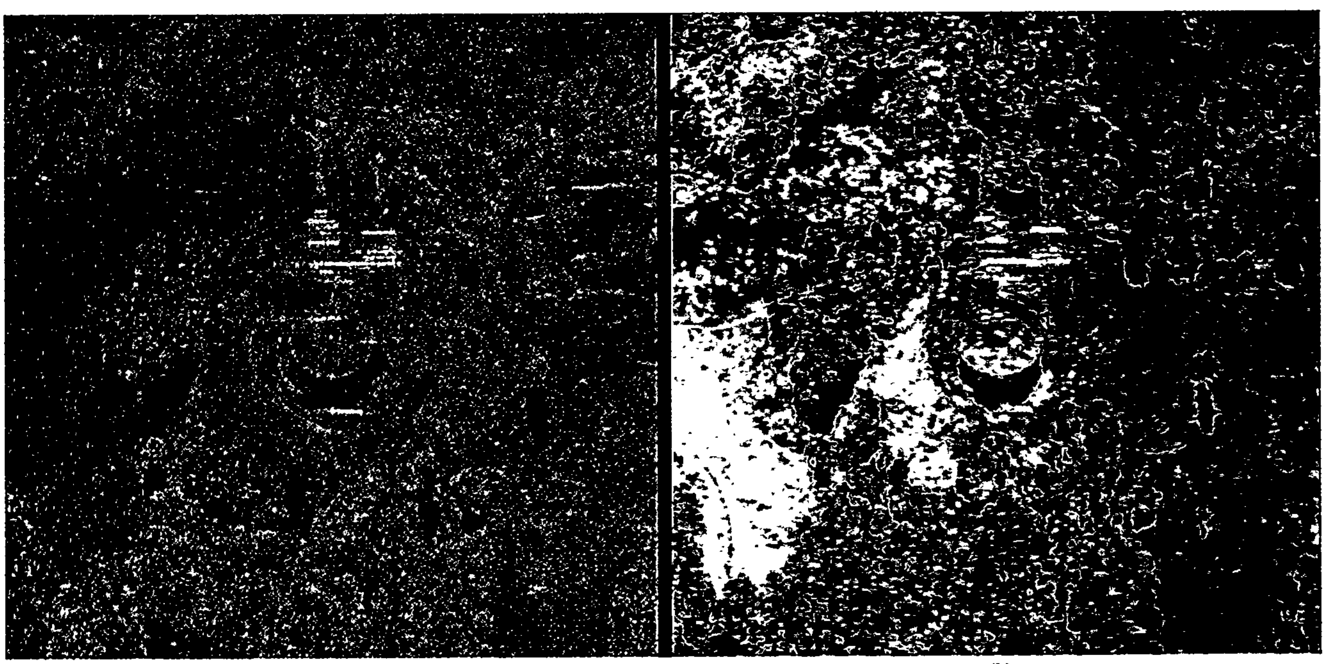

(a) (b)

Figure 4-a) Log-enhanced SAR magnitude image of a storage tank. b) Coherence map of the storage tank employing the airplane belly and wing antenna (small baseline).

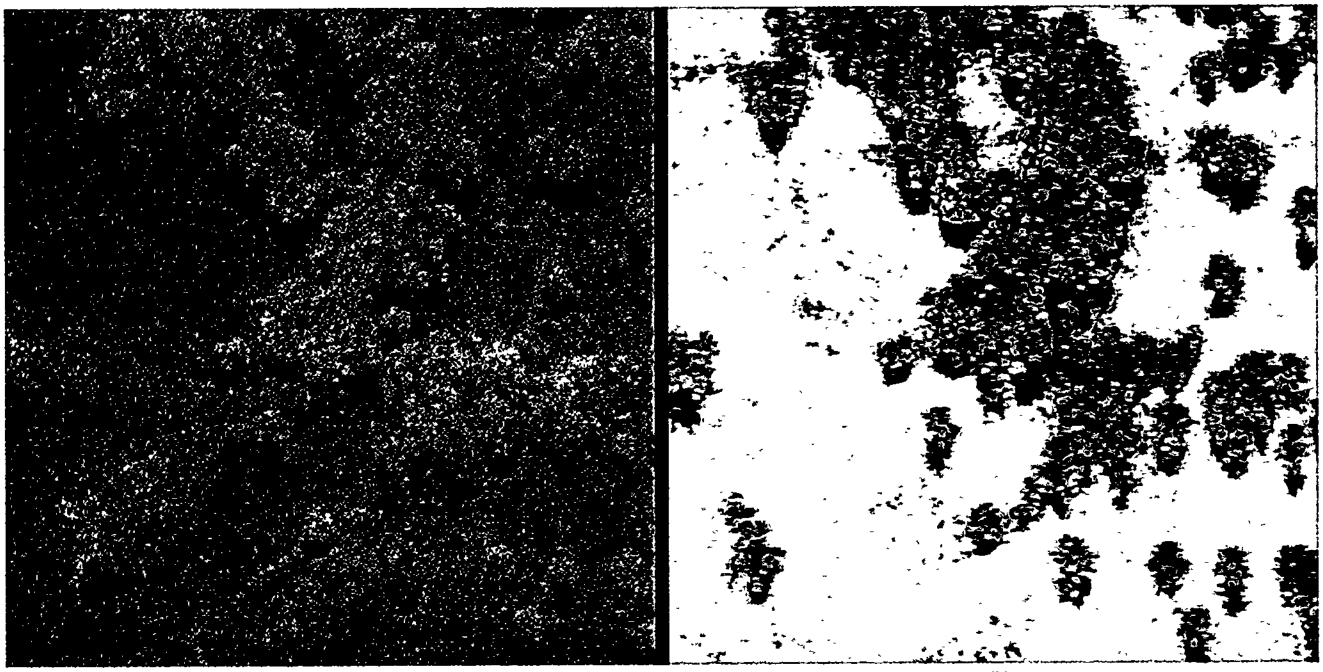

(a) (b)

Figure 5-a) Log-enhanced SAR magnitude image of tree canopies. b) Coherence map of the tree canopies with small baseline.

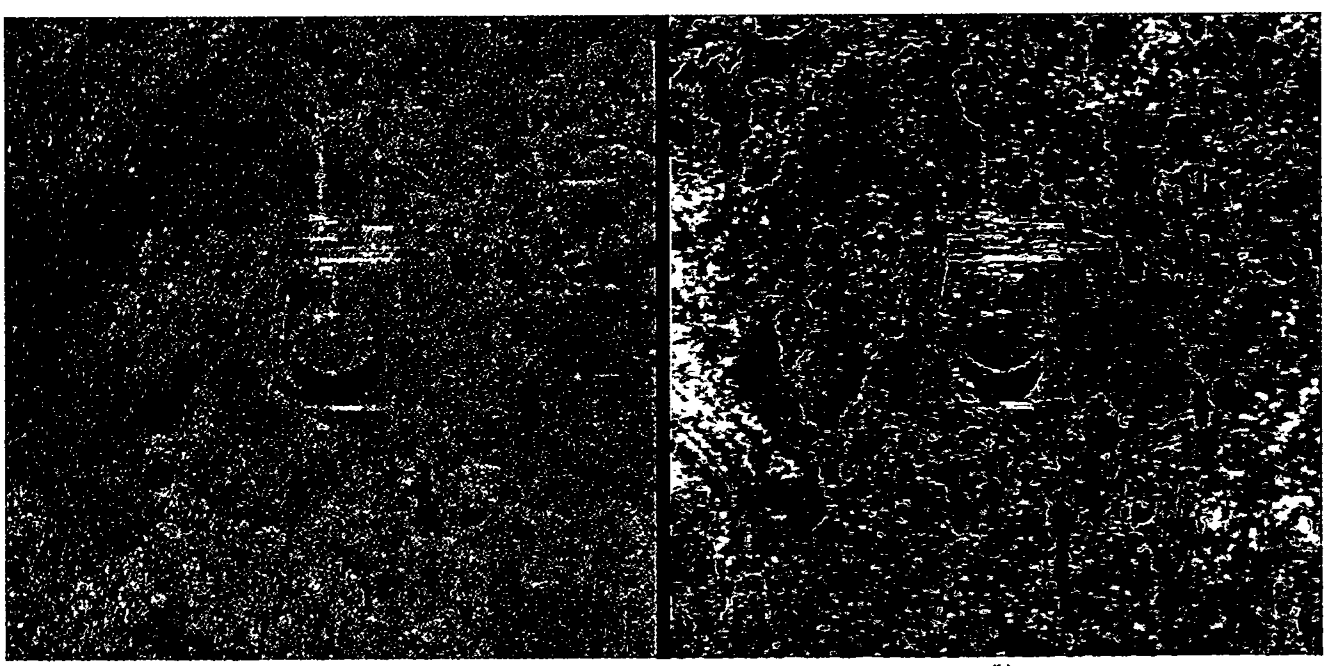

(a) (b)

Figure 6-a) Log-enhanced SAR magnitude image of a storage tank. b) Coherence map for same storage tank. The baseline is two wing antennas (large baseline).

ACKNOWLEDGEMENTS

This work was supported by the United States Department of Energy under Contract DE-AC04-94AL85000 and Department of Energy NN-20 research monies. Sandia is a multiprogram laboratory operated by Sandia Corporation, a Lockheed Martin Company, for the United States Department of Energy.

REFERENCES

1. L. C. Graham, "Synthetic interferometer radar for topographic mapping," *Proc. of IEEE*, **62**, pp. 763-768, 1974.
2. H. A. Zebker and R. M. Goldstein, "Topographic mapping from interferometric synthetic radar observations," *J. Geophys. Res.*, **91** pp. 4993-4999, 1986.
3. H. Hirosawa and N. Kobayashi, "Terrain height measurement by synthetic aperture radar with an interferometer," *Int. J. Remote Sensing*, **7**, pp. 339-348, 1986.
4. F. K. Li and R. M. Goldstein, "Studies of multibaseline spaceborne interferometric synthetic aperture radars," *IEEE Trans on Geosci. and Remote Sensing*, **28**, pp. 88-97, 1990.
5. L. Gray and P. J. Farris-Manning, "Repeat-pass interferometry with airborne synthetic aperture radar," *IEEE Trans. on Geosci. and Remote Sensing*, **31**, pp. 180-191, 1993.
6. C. V. Jakowatz, Jr., D. E. Wahl, P. H. Eichel, D. C. Ghiglia, and P. A. Thompson, *Spotlight-mode Synthetic Aperture Radar: A Signal Processing Approach,* Kluwer Academic Publishers, Boston, 1996.
7. D. A. Yocky and B. F. Johnson, "Repeat-pass dual-antenna synthetic aperture radar interferometric change-detection post-processing," *Photogram. Eng. And Remote Sensing*, **64**, pp. 425-429, 1998.
8. J. O. Hagberg, L. M. H. Ulander, and J. Askne, "Repeat-pass SAR interferometry over forested terrain," *IEEE Trans. on Geosci. and Remote Sensing*, **33**, pp. 331-340, 1995.
9. U. Wegmuller, C. Werner, "Retrieval of vegetation parameters with SAR interferometry," *IEEE Trans. on Geosci. and Remote Sensing*, **35**, pp. 18-24, 1997.
10. H. Askne, P. B. G. Dammert, L. M. H. Ulander, and G. Smith, "C-band repeat-pass interferometric SAR observations of the forest," *IEEE Trans. on Geosci. and Remote Sensing*, **35**, pp. 25-35, 1997.
11. D. A. Yocky, "Interferometric SAR coherence classification utility assessment," *Proc. of IGARSS '98*, Vol. IV, pp. 1784-1786, IEEE, Seattle, WA, 1998.
12. W. Goodman, *Statistical Optics,* John Wiley & Sons, New York, 1985.
13. D. L. Bickel, W. H. Hensley, and D. A. Yocky, "The effect of scattering from buildings on interferometric SAR measurement," *Proc. of IGARSS '97*, Vol. IV, pp. 1545-1547, IEEE, Singapore, 1997.
14. H. A. Zebker, and J. Villasenor, "Decorrelation in interferometric radar echoes," *IEEE Trans on Geosci. and Remote Sensing,* **30**, pp. 950-959, 1992.